Biosensors and Bioelectronics 165 (2020) 112358

Contents lists available at ScienceDirect

Biosensors and Bioelectronics

journal homepage: http://www.elsevier.com/locate/bios

Electrochemically controlled grafting of polymers for ultrasensitive electrochemical assay of trypsin activity

Qiong Hu [a,b], Yu Bao [a], Shiyu Gan [a], Yuwei Zhang [a,**], Dongxue Han [a,b], Li Niu [a,b,c,*]

[a] Center for Advanced Analytical Science, School of Chemistry and Chemical Engineering, Guangzhou University, Guangzhou, 510006, PR China
[b] School of Civil Engineering, Guangzhou University, Guangzhou, 510006, PR China
[c] Collaborative Innovation Center of Tumor Marker Detection Technology, Equipment and Diagnosis-Therapy Integration in Universities of Shandong, Shandong Province Key Laboratory of Detection Technology for Tumor Makers, School of Chemistry and Chemical Engineering, Linyi University, Linyi, 276005, PR China

ARTICLE INFO

Keywords:
Electrochemical biosensor
Protease
Trypsin activity
Electrochemically controlled grafting
Signal amplification
Inhibitor screening

ABSTRACT

As one of the most important proteolytic enzymes, trypsin is useful as a reliable and specific biomarker for the diagnosis of pancreatitis and other pathological conditions. In this paper, a novel signal-on electrochemical biosensor based on the use of electrochemically controlled grafting of polymers as an amplification strategy is described for the ultrasensitive assay of trypsin activity. The carboxyl-group-free peptide, serving as the substrate for the recognition of trypsin, is first immobilized via its N-terminus. The tryptic cleavage of peptide substrate can generate a free carboxyl group at the C-terminus of the truncated peptide, to which through the carboxylate-Zr(IV)-carboxylate linkage the carboxyl-group-containing initiator for atom transfer radical polymerization (ATRP) can be conjugated. The subsequent surface-initiated grafting of polymers (SI-GOP) based on electrochemically controlled ATRP (eATRP), with ferrocenylmethyl methacrylate (FcMMA) as the monomer, can bring a large amount of Fc tags to electrode surface, resulting in the generation of a very high detection signal. The eATRP-based SI-GOP is easy to operate and low-cost as an amplification strategy. Under optimal conditions, the detection limit for trypsin activity can be down to 0.016 mU mL^{-1} (~2.68 pM or ~0.064 ng mL^{-1}). As the current signal increases with trypsin activity, this trypsin biosensor is less susceptible to false positives due to the signal-on mode. Moreover, it is highly selective and applicable to inhibitor screening and the assay of trypsin activity in the presence of complex biological matrices. Taking together, this electrochemical trypsin biosensor may hold great potential in diagnostic applications.

1. Introduction

Trypsin is one of the most important serine proteases in the digestive system of many vertebrates for protein digestion. As an endopeptidase, it catalyzes the cleavage of peptide bonds predominantly at the carboxyl side of the arginine or lysine residue (Keil, 1971). It is formed in the small intestine when the zymogen trypsinogen, secreted by the pancreas, is activated by enteropeptidase (Keil, 1971). Trypsin is the most frequently used enzyme in mass spectrometry (MS)-based proteomics (Aebersold and Mann, 2003). Besides, abnormal levels of trypsin are associated with various pathological conditions such as acute and chronic pancreatitis, cystic fibrosis, and pancreatic, ovarian, gastric, and biliary tract cancers. For example, the serum trypsin concentration in healthy individuals ranges from 138 to 406 ng mL^{-1}, whereas in the subjects suffering from acute pancreatitis it ranges from 970 to 6500 ng mL^{-1} (Elias et al., 1977). Therefore, the assay of trypsin activity and inhibitor screening are integral to trypsin-related proteomic, diagnostic, and therapeutic applications.

To date, a variety of methods using synthetic substrates as the biorecognition elements have been described for the assay of trypsin activity (Bi et al., 2009; Goldberg et al., 2014; Zeng et al., 2015). In addition to the electrophoretic (Lefkowitz et al., 2010), colorimetric (He et al., 2019a; Zaccheo and Crooks, 2011), fluorescent (Algar et al., 2012; Wang et al., 2010, 2014; Zauner et al., 2011), phosphorescent (Wu et al., 2014), electrochemiluminescent (ECL) (Cheng et al., 2018), chemiluminescent (CL) (Zhang et al., 2014), photoelectrochemical (PEC) (Dai

* Corresponding author. Center for Advanced Analytical Science, School of Chemistry and Chemical Engineering, Guangzhou University, Guangzhou, 510006, PR China.
** Corresponding author.
E-mail addresses: ccywzhang@gzhu.edu.cn (Y. Zhang), lniu@gzhu.edu.cn (L. Niu).

https://doi.org/10.1016/j.bios.2020.112358
Received 8 April 2020; Received in revised form 26 May 2020; Accepted 1 June 2020
Available online 4 June 2020

et al., 2017), mass spectrometric (MS) (Hu et al., 2015), and the surface enhanced Raman scattering (SERS)- (Chen et al., 2013; Wu et al., 2015), quartz crystal microbalance (QCM)- (Stoytcheva et al., 2013), cantilever- (Raorane et al., 2008), and nanopore-based methods (Zhou et al., 2016), several electrochemical trypsin biosensors have also been reported (Adjemian et al., 2010; Cao et al., 2013; González-Fernández et al., 2016; Liang et al., 2014), in view of their rapid response, minute sample volume, high sensitivity and selectivity, low cost, etc. Electrochemical assay of trypsin activity can be operated based on the tryptic cleavage of methylene blue (MB) (González-Fernández et al., 2016) or ferrocene (Fc) (Adjemian et al., 2010; Anne et al., 2012) tagged substrates, because the cleavage event can result in the release of electroactive tags. Although very easy to operate, such assays are suffered from two defects: the susceptibility to false positives (due to the signal-off mode, in which the release of electroactive tags could be due to events other than the tryptic cleavage (e.g., the desorption of the end-tethered substrates)) and the unsatisfactory sensitivity (one substrate is conjugated with only a tag). The former defect can be effectively avoided provided that the electroactive tags could be introduced after the substrate cleavage (Cao et al., 2013), and the latter is routinely bypassed based on the use of signal amplification strategies (Liang et al., 2014). Despite these advances, relatively little progress has been achieved toward the important goal of developing an easy-to-operate and low-cost electrochemical biosensor for the signal-on assay of trypsin activity at very low levels.

Surface-initiated grafting of polymers (SI-GOP) via free-radical polymerization has in recent years emerged as an attractive strategy for signal amplification (Hu et al., 2020b; Kim and Sikes, 2020; Sikes et al., 2008; Wu et al., 2012). Through the side chains of the grafted polymers, hundreds to millions of signal tags can be conjugated for signal output (Hu et al., 2019; Wu et al., 2009, 2010); also, the opacity, thickness, and color of the resulting polymer spots can serve as a detection signal (He et al., 2008, 2019b; Kim and Sikes, 2019). In particular, SI-GOP based on atom transfer radical polymerization (ATRP), a versatile reversible deactivation radical polymerization (RDRP) proposed by the groups of Matyjaszewski (Wang and Matyjaszewski, 1995) and Sawamoto (Kato et al., 1995) in 1995, has attracted considerable attention in the sensitive assay of clinically relevant targets ranging from nucleic acids and proteins to antigens (Hu et al., 2017, 2018; Lou et al., 2005; Yuan et al., 2012). For example, it was used by Lou et al. (2005) as an amplification strategy in visual DNA assay and a limit of detection (LOD) of 1.0 nM was obtained. In this study, the ATRP-initiator-labeled detection probes were first tethered to the target DNA fragments localized sites via a two-step biorecognition reaction, and subsequently the ATRP-based SI-GOP in the presence of 2-hydroxyethyl methacrylate (HEMA) as the monomer led to the formation of the opaque polymer spots, which are discernible to the naked eye. The growing use of the ATRP-based SI-GOP for signal amplification is prompted by the following merits of ATRP: (1) it is biologically friendly and through it various functional polymers (e.g., DNA- and protein-polymer bioconjugates) have been prepared (Boyer et al., 2016); (2) it is applicable to the highly efficient polymerization of many monomers in aqueous solutions and under mild conditions (Matyjaszewski and Tsarevsky, 2014); and (3) its "living" character allows control over the length of polymer chains, such that the amplification degree is tunable. As the ATRP-based SI-GOP involves only two steps (i.e., the tethering of ATRP initiators and the succedent ATRP reaction), it is easy to operate and low-cost as an amplification strategy. However, radicals are sensitive to oxygen. Deoxygenation by such as continuous inert-gas purging during the grafting process may be sometimes not friendly to operate. For this reason, various oxygen-tolerant versions of the ATRP-based SI-GOP have been harnessed for signal amplification. As an example, the electrochemically controlled ATRP (eATRP)-based SI-GOP has recently been described by us as an amplification strategy in the electrochemical assay of DNA (Hu et al., 2017) and protein kinase (Hu et al., 2018). In the eATRP-based SI-GOP, the dissolved oxygen can be consumed up by a portion of the Cu^{I} activators, which are continuously generated from electrochemical reduction of the air-stable Cu^{II} deactivators. As a result, the eATRP-based SI-GOP is tolerant to oxygen, thus showing great promise as an amplification strategy.

By taking advantage of the eATRP-based SI-GOP as an amplification strategy, we show herein an easy-to-operate and low-cost electrochemical biosensor for the signal-on assay of trypsin activity. The fabrication of the trypsin biosensor involves the tethering of the carboxyl-group-free peptide substrates to the surface of a gold electrode via the N-terminal Cys residue, the cleavage of substrates by trypsin, the conjugation of carboxyl-group-containing initiators to the C-terminus of the truncated peptides via the Zr(IV) linkers, and the eATRP-based SI-GOP with ferrocenylmethyl methacrylate (FcMMA) as the monomer. Clearly, a higher level of trypsin activity will result in the output of a higher detection signal, leading to a signal-on assay of trypsin activity. Through the eATRP-based SI-GOP, in addition, a large amount of Fc tags can be introduced for signal output. The described electrochemical biosensor thus shows great promise for the signal-on assay of trypsin activity at very low levels.

2. Material and methods

2.1. Materials and reagents

Peptide substrate, Cys-Gly-Gly-Ser-Ser-Arg-Gly-Gly-$CONH_2$ (CGGSSRGG-$CONH_2$), with purity $\geq$ 95% was provided by Shanghai Science Peptide Biological Technology Co. Ltd. (Shanghai, China). Trypsin from porcine pancreas (specific activity, 250 U mg^{-1}; MW, 23.8 kDa) and chymotrypsin were supplied by Sangon Biotech (Shanghai) Co. Ltd. (Shanghai, China). Cytochrome c from bovine heart, 6-mercapto-1-hexanol (MCH), pepsin from porcine gastric mucosa, FcMMA, Ru$(NH_3)_6Cl_3$, $ZrOCl_2$, hemoglobin human, and Bowman-Birk inhibitor (BBI) from soybean were purchased from Sigma-Aldrich. Normal human serum (NHS), $LiClO_4$, γ-globulin, and thrombin from bovine plasma were offered by YiJi Industrial Co. Ltd. (Shanghai, China), Aladdin Bio-Chem Technology Co. Ltd. (Shanghai, China), Yuanye Biotechnology Co. Ltd. (Shanghai, China), and Solarbio Science & Technology Co. Ltd. (Beijing, China), respectively. α-Bromophenylacetic acid (BPAA), albumin from bovine serum (BSA), ferrocenecarboxylic acid (FcCOOH), tris (hydroxymethyl)aminomethane (Tris), KPF_6, $CuBr_2$, and tris[2-(dimethylamino)ethyl]amine (Me_6TREN) were supplied by J&K Scientific Ltd. (Shanghai, China). *N*,*N*-Dimethylformamide (DMF), $CaCl_2$, absolute ethanol (EtOH), and other chemicals were offered by Sinopharm Chemical Reagent Co. Ltd. (Shanghai, China). All chemicals were used as supplied. Ultrapure water ($\geq$18.25 MΩ cm) was from a Millipore Milli-Q system.

2.2. Apparatus

Cyclic voltammetry (CV), amperometric i-t curve, square-wave voltammetry (SWV), electrochemical impedance spectroscopy (EIS), and linear sweep voltammetry (LSV) were carried out at room temperature with a three-electrode system: a modified polycrystalline gold working electrode (Φ = 3.0 mm), a saturated calomel electrode (SCE, reference electrode), and a platinum wire counter electrode. Voltammetric experiments and i-t curve were performed with a CHI 760 E electrochemical workstation (CH Instruments). EIS analyses were carried out at the open circuit potential (OCP) using a Reference 600+ potentiostat (Gamry Instruments), with the frequency range from 10^5 to 10^{-1} Hz and a potential amplitude of 10 mV, in the presence of 5.0 mM $[Fe(CN)_6]^{3-/4-}$ in 0.1 M KNO_3. A field emission scanning electron microscope (JSM-7100 F, JEOL) equipped with energy-dispersive X-ray spectroscopy (EDS) was used to collect the scanning electron microscopy (SEM) images (accelerating voltage, 15 kV) and the elemental mappings. Atomic force microscopy (AFM) images were collected in tapping mode using Nanosurf FlexAFM.

2.3. Electrochemical assay of trypsin activity

After a pretreatment according to the procedures described elsewhere (Hu et al., 2017, 2019), onto the clean gold electrode surface the peptide substrate aqueous solution (1.5 μM, 10 μL) was added. Then, the electrode surface was incubated for 45 min at 37 °C, rinsed rigorously with ultrapure water, blocked with 2.0 mM MCH in 60% EtOH for 15 min at 37 °C, and rinsed with EtOH and ultrapure water. After this, 10 μL of trypsin solution (50 mM Tris-HCl, 1.0 mM $CaCl_2$, pH 7.6) or 10 μL of the synthetic samples (prepared by spiking trypsin solutions into undiluted NHS, and the shares of NHS in the final solutions were 5%) was added to the electrode surface, followed by an incubation for 1.0 h at 37 °C and a rigorous rinse with ultrapure water. Subsequently, the electrode surface was soaked in 5.0 mM $ZrOCl_2$ in 20% EtOH for 30 min at 37 °C, rinsed with ultrapure water, soaked in 1.0 mM BPAA in 40% EtOH for 30 min at 37 °C, and rinsed with copious EtOH and ultrapure water. The electrode surface was then soaked in the eATRP solution (prepared by sequentially adding 0.1 mL of 10 mM $CuBr_2$/Me_6TREN in DMF, 0.1 mL of 10 mM FcMMA in DMF, 1.0 mL of 1.0 M KBr, and 6.0 mL of 0.1 M KPF_6 into 2.8 mL of DMF), followed by the eATRP-based SI-GOP for 30 min under a potentiostatic condition using i-t curve. Last, the electrode surface was treated with LSV (initial potential, 0 V; final potential: 0.2 V) for several times (to remove the possible Cu(0) residue), rinsed rigorously with EtOH and ultrapure water (to remove any physically adsorbed species), and analyzed with SWV (increase potential, 4.0 mV; potential amplitude, 25 mV; quiet time, 15 s) in 0.5 M $LiClO_4$.

3. Results and discussion

3.1. Principle of the trypsin activity assay

The assay principle is illustrated in Scheme 1. Although the presence of trypsin can be specifically probed by using molecularly imprinted polymers (MIPs) (Ertürk et al., 2016), antibodies (Park et al., 2016), or synthetic substrates (Adjemian et al., 2010) as the biorecognition elements, only the substrate-based methods are suitable for activity assay. Herein, the octopeptide CGGSSRGG-$CONH_2$ is used as the substrate, which has been designed such that it is free of carboxyl group and can be tethered to gold electrode surface via its N-terminus. In the presence of trypsin, the peptide substrate is cleaved specifically at the carboxyl side of Arg residue, leaving a carboxyl-group-containing fragment (CGGSSR-COOH) on the electrode surface. Through the robust carboxylate-Zr(IV)-carboxylate linkage (Hu et al., 2018), the ATRP initiator BPAA can then be conjugated to the electrode surface. The eATRP-based SI-GOP is initiated by the Cu^I/Me_6TREN activators, which are continuously (re)generated from in situ electrochemical reduction of the air-stable $Cu^{II}Br$/Me_6TREN deactivators (Hu et al., 2017; Magenau et al., 2011). The activators react initially with the initiators to form the deactivators and the initiating radicals, which are capable of repeated monomer addition to form the propagating radicals (i.e., the active species) or the Br-capped dormant species by reacting with the deactivators. The propagation of the active species eventually results in the grafting of long polymer chains, bringing a large amount of Fc tags to the electrode surface, allowing the assay of trypsin activity even at very low levels. The eATRP-based SI-GOP avoids the need for costly and complicated catalytic or nano labels; thus, it is easy to operate and low-cost as an amplification strategy. It is also clear that a higher level of trypsin activity can eventually result in the introduction of a higher amount of Fc tags. Thus, the highly sensitive assay of trypsin activity in a signal-on mode can be realized by using peptide as the biorecognition element and the eATRP-based SI-GOP for signal amplification.

3.2. Characterizations

In this work, the activators for the eATRP-based SI-GOP were generated from potentiostatic reduction of the deactivators. To ascertain the reduction potential, the electrochemical properties of the redox couple were studied. Fig. S1 shows the CV curve of the initiator-modified electrode in the monomer-free eATRP solution. As can be seen, the reduction peak is located at −0.55 V vs. SCE. The Nernst equation of the redox couple can be expressed as:

$$E_{app} = E^{\circ\prime} + \frac{RT}{nF}\ln\frac{C_{[Cu^{II}Br/L]}}{C_{[Cu^{I}/L]}} \quad (1)$$

where E_{app}, the potential applied; $E^{\circ\prime}$, the apparent formal potential of the redox couple; F, the Faraday constant; R, the universal gas constant; L, Me_6TREN. Clearly, the concentration of the activator and thus the grafting rate of polymer chains is dictated by the E_{app}; namely, the eATRP-based SI-GOP can be precisely controlled by the E_{app}. In this work, the eATRP-based SI-GOP was operated at −0.6 V.

To demonstrate the feasibility of the trypsin activity assay, the response signals of the differently modified electrodes were collected. In this work, the organometallic compound Fc, which has superior stability and redox properties, was served as the electroactive tag. It is in expectation that when Fc tags are present on the electrode surface, a well-defined waveform corresponding to the electrochemical oxidation of Fc tags into the ferrocenium cations should be observed. As shown in Fig. 1A, for the electrode modified without trypsin, no clear oxidation current can be observed. This is in expectation because no functional sites are available to conjugate initiators, unless the peptide substrates have been cleaved by trypsin. In the absence of initiators, undoubtedly,

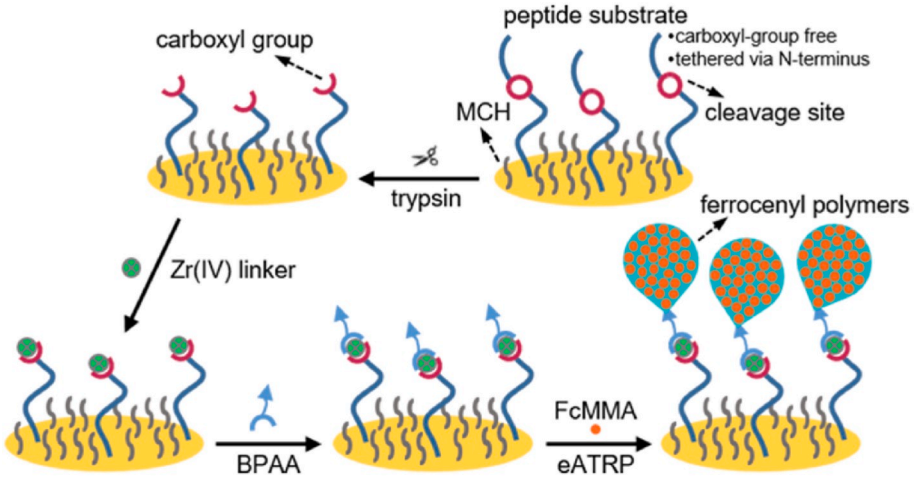

Scheme 1. Schematic illustration of the electrochemical assay of trypsin activity.

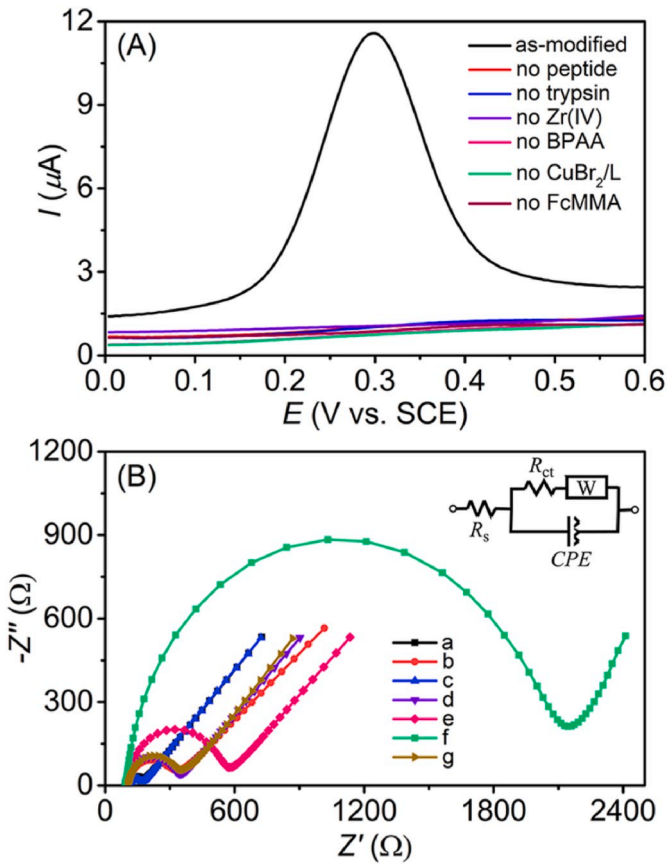

Fig. 1. (A) SWV curves of the differently modified electrodes. (B) Nyquist plots of gold electrode (a) and of those after the stepwise treatment with peptide substrate (b), MCH (c), trypsin (d), Zr(IV) linker (e), ATRP initiator (f), and the eATRP-based SI-GOP (g). Inset shows the equivalent circuit (*W*, Warburg resistance; R_s, solution resistance; *CPE*, constant-phase element). Trypsin, 210 μU mL^{-1}. (For interpretation of the references to color in this figure legend, the reader is referred to the Web version of this article.)

no polymer chains can be grafted from the electrode surface. Similarly, no clear oxidation peak can be observed for the electrodes modified without peptide substrates, Zr(IV) linkers, initiators, deactivators, or monomers. In this work, trypsin was specifically recognized based on the enzyme-substrate interactions and all other components (e.g., Zr(IV) linker, initiator, and monomer) were tethered to the electrode surface via a site-specific manner. Additionally, the blocking of the vacant sites on electrode surface with MCH and the vigorous rinse after each modification can also effectively remove the nonspecifically adsorbed species. As a result, the nonspecific adsorption of these components on electrode surface is negligible. For the perfectly modified electrode, as expected, a high oxidation peak occurred at ~0.3 V vs. SCE. The confinement of Fc tags on electrode surface was evidenced by the scan rate-dependent CV curves, shown in Fig. S2. The peak currents (I_{pa} and I_{pc}) of the Fc redox reaction are directly proportional to the scan rates (inset, Fig. S2), in line with the surface-confined redox process (Hu et al., 2017). The polymers present on the electrode surface were confirmed by the SEM (Figs. S3 and A) and AFM images (Fig. S4). As can be seen from Fig. S3,B-D, the Zr(IV) linkers, ATRP initiators, and Fc tags were all present on the electrode surface. Taking together, the electrochemical assay of trypsin activity is feasible and reliable. As calculated, the signal-to-noise ratio (SNR), with or without the addition of 210 μU mL^{-1} trypsin, was ca. 70.43. The high SNR arises from two aspects: (1) the eATRP-based SI-GOP can bring a large amount of Fc tags to the electrode surface and thus result in the generation of a high oxidation current, and (2) the blocking of the vacant sites with MCH can effectively suppress the background current (Hu et al., 2019). In this work, the peptide substrates were immobilized via Au–S bonds. The coverage (Γ) of peptide substrate can affect the cleavage efficiency. To obtain the Γ value, the end-tethered substrates were desorbed from electrode surface by LSV (Hu et al., 2018, 2019), illustrated in Fig. S5. The Γ value can be calculated from the expression $\Gamma = Q/\nu FA$, where Q is the integral area of the desorption wave (~0.0204 μA V, plot "a"), ν is the scan rate (0.02 V s^{-1}), F is the Faraday constant (96485.33 C mol^{-1}), and A is the electrode surface (0.071 cm^2). The Γ value is estimated to be ~0.15 nmol cm^{-2}, indicating that ~71% of the added peptides (1.5 μM, 10 μL) have been end-tethered. In addition, the maximal Γ value for peptide substrate was found to be ~0.39 nmol cm^{-2} (plot "b"; Q, ~0.0537 μA V), indicating that ~38.5% of the binding sites have been occupied by the peptide substrates. A low Γ value is favorable to the tryptic cleavage, since in such case the steric hindrance will be moderate. From this expression, the amount of Fc tags can also be estimated (here, Q is the integral area (~1.4452 μA V) of the oxidation wave of the SWV curve in Fig. 1A and ν is the scan rate of SWV (0.06 V s^{-1})). Accordingly, the amount of Fc tags is estimated to be ~3.52 nmol cm^{-2}. The amount of the cleaved peptides was determined to be ~12.0 pM cm^{-2} (corresponding to a cleavage yield of ~8.0% of the end-tethered peptides), by measuring the amount of $Ru(NH_3)_6^{3+}$ that is required to completely compensate the negative charges of the carboxyl termini (Fig. S6). As calculated, the average number of Fc tags conjugated to each cleaved peptide substrate can be as high as ~293.3.

The modification of electrode surface was tracked stepwise by EIS. Representative Nyquist plots are shown in Fig. 1B. For the clean surface (plot "a"), the charge-transfer resistance (R_{ct}) was ~73.8 Ω, signifying the fast charge-transfer kinetics. After tethering of peptide substrates (plot "b"), the R_{ct} increased to ~234.9 Ω, resulting from the steric hindrance from the peptide layer (Hu et al., 2020a). The backfilling of the vacant sites with MCH brought the R_{ct} to ~60.2 Ω (plot "c"), because the MCH layer can force the peptide substrates to rearrange into an upright configuration (a low coverage and the nonspecific interactions with electrode surface allow them in a flat-lying configuration), of which the steric hindrance is moderate (Hu et al., 2020a). Notably, the value is lower than that of the clean surface, implying that when the end-tethered peptide substrates are in an upright configuration they can facilitate the charge transfer, likely due to the presence of the positively-charged Arg residues. The cleavage of peptide substrates by trypsin brought the R_{ct} to ~237.9 Ω (plot "d"), which is in expectation because the carboxyl groups are electrostatically repulsive to the negatively charged $[Fe(CN)_6]^{3-/4-}$ (Hu et al., 2020a). After the modification of Zr(IV) linkers (plot "e") and ATRP initiators (plot "f"), the R_{ct} increased to ~455.5 Ω and ~1944 Ω, respectively, which are consistent with the previous reports (Hu et al., 2017, 2018). As can be seen, after the eATRP-based SI-GOP, the R_{ct} dropped to ~244.2 Ω (plot "g"), indicative of the presence of a large amount of Fc tags, which can greatly facilitate the interfacial charge transfer (Hu et al., 2020a). Taking together, it can be concluded that the modification of the electrode surface proceeded as expected.

3.3. Analytical performance

To improve the assay sensitivity, the eATRP-based SI-GOP was taken advantage of as an amplification strategy, in view of its ease in operation and low cost. Clearly, the presence of a higher level of trypsin activity can result in the cleavage of more peptide substrates and thus the generation of more carboxyl termini; as a result, a higher amount of Fc tags can be brought to the electrode surface. With this in mind, the described trypsin biosensor is expected to be applicable to the quantitative assay of the proteolytic activity of trypsin. To evaluate its analytical performance, the activity-dependent SWV curves were collected. As the growth of polymer chains is accompanied by the continuous introduction of Fc tags, a longer grafting time can result in a higher current signal. For a short turnaround time, in the proof-of-concept experiment,

the grafting time was set to 30 min. The SWV curves and the corresponding calibration curve of the peak current versus trypsin activity, from 30 to 210 μU mL^{-1}, are shown in Fig. 2A. As can be seen, the peak current increased linearly with the increase of trypsin activity from 30 to 210 μU mL^{-1}, and the "signal-on" mode is less susceptible to false positives (the desorption of the end-tethered peptide substrates, for example, would not result in the introduction of Fc tags). The linear regression equation of the calibration curve can be expressed as I_p (μA) $= 0.045\,A_{trypsin} + 0.156$, where $A_{trypsin}$ is the trypsin activity in μU mL^{-1}, with a correlation coefficient of 0.998. The LOD, as calculated based on the $3\sigma_b$/slope criterion (σ_b, the standard deviation of the control) (Long and Winefordner, 1983), is 0.016 mU mL^{-1} (molarity, ~2.68 pM; mass concentration, ~0.064 ng mL^{-1}). Such a high sensitivity can be ascribed to the eATRP-based SI-GOP, through which the detection signal can be significantly amplified. A detailed comparison of the analytical performance of different methods is summarized in Table S1. As can be seen, the LOD is comparable to or significantly lower than that of other methods. For example, it has been lowered by nearly two orders of magnitude (~2.68 pM vs 250 pM), when compared with that of the method based on the tryptic cleavage of the MB-tagged peptide substrates (González-Fernández et al., 2016). In the MB-based method, the cleavage of one peptide substrate corresponded to the release of an MB tag. In our assay, instead, it would result in the grafting of a long polymer chain that contains many Fc tags. As a result, the LOD can be significantly lowered. Besides, compared with the method in which one carboxyl terminus was conjugated with only an Fc tag (for details, please see Fig. S7), the LOD can be lowered by ~107-fold (~2.68 pM vs 286.4 pM). The assay reproducibility is also satisfactory. In the presence of 210 μU mL^{-1} trypsin, for example, the intra- and inter-coefficients of variation of the peak current of five repeated assays were 5.2% and 5.7%, respectively. These results demonstrate that the described biosensor is applicable to the highly sensitive assay of trypsin activity.

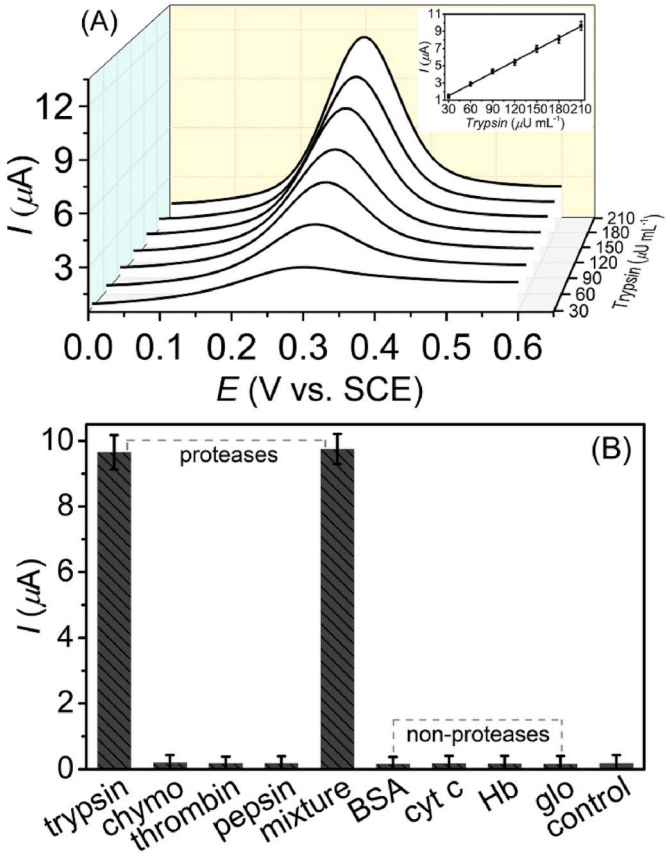

Fig. 2. (A) SWV curves toward different levels of trypsin activity (30, 60, 90, 120, 150, 180, 210 μU mL^{-1}). Inset depicts the calibration curve of peak current versus trypsin activity. (B) Peak currents toward four different proteases, a mixture of them, four different non-proteases, and the blank control. Trypsin, 0.84 ng mL^{-1}; others, 10 ng mL^{-1}.

To test the long-term stability, the perfectly-modified electrodes (treated with 210 μU mL^{-1} trypsin) were stored at 4 °C or at room temperature. After two weeks, the peak currents were collected. As shown in Fig. S8, no significant decreases (decreased by ~3.83% or ~4.09% for a two-week storage at 4 °C or at room temperature, respectively) in peak current were observed for both cases, indicative of the satisfactory long-term storage stability.

3.4. Selectivity and practicability

To assay trypsin activity, peptide substrate was used herein as the biorecognition element. Peptides as biorecognition elements offer three additional benefits: low cost, ease in synthesis and modification in large scales, and superior chemical/thermal stability. To assess the assay selectivity, the peak currents derived from four proteases (trypsin, chymotrypsin (chymo), thrombin, and pepsin), a mixture of them, and four non-proteases (BSA, cytochrome c (cyt c), hemoglobin (Hb), and γ-globulin (glo)) were collected, as shown in Fig. 2B. In the proof-of-concept experiment, the concentration of trypsin was 0.84 ng mL^{-1}, and of others was 10 ng mL^{-1}. As seen, the presence of these interferents did not interfere with the assay of trypsin activity, indicating that the peptide substrate is unresponsive to these interferents. The high selectivity is in expectation, because the enzyme-substrate interactions are highly specific in terms of the recognition sites and the reaction conditions (e.g., the optimal pH).

The influence of complex biological matrices on the response signal was evaluated based on the recovery assays, using 20-fold diluted NHS as the model matrix. The recoveries and relative standard deviations (RSDs) of the standard addition assays are shown in Table 1. The recoveries for the three samples were from ~96.3% to ~105.4%, with the RSD ranging from 5.2% to 5.6%. The satisfactory anti-interference capability indicates that the trypsin biosensor is applicable to the assay in the presence of complex biological matrices.

3.5. Potential application in inhibitor screening

Up-regulated level of trypsin activity is known to be an aggravating factor of many pathological conditions (e.g., acute pancreatitis). In recent years, trypsin inhibitors as therapeutic drugs have attracted considerable research interest in targeted therapy. To illustrate that the trypsin activity assay can also be applied to the screening of inhibitors, BBI from soybean was tested as the model (Gu et al., 2011). The electrodes were modified as described in the Material and methods, except that the trypsin solutions were incubated with certain doses of BBI for 15 min prior to their addition to electrode surface. Because of the retardation of the cleavage of peptide substrates by trypsin, a lower current signal is expected toward a higher inhibitor dose. One can see from Fig. 3 that a higher BBI dose will result in a lower peak current. The IC_{50} value (the half-maximal inhibitory dose) of BBI, estimated from the dose-dependent inhibition efficiency curve (inset, Fig. 3), is 4.18 ng mL^{-1} toward the 210 μU mL^{-1} trypsin. These results show that the trypsin activity assay can be applied to inhibitor screening.

Table 1
Assay of trypsin activity in spiked 5% NHS.

sample	added (μU mL^{-1})	found (μU mL^{-1})	recovery (%)	RSD (%, n = 5)
1	30	30.7	~102.3	5.6
2	120	126.5	~105.4	5.4
3	210	202.3	~96.3	5.2

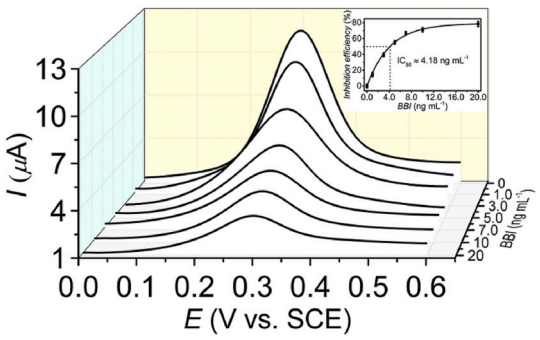

Fig. 3. SWV curves in the presence of different doses of BBI (0, 1.0, 3.0, 5.0, 7.0, 10, 20 ng mL^{-1}). Inset depicts the curve of inhibition efficiency versus BBI dose. Trypsin, 210 μU mL^{-1}.

4. Conclusions

In summary, an easy-to-operate and low-cost electrochemical biosensor based on the use of a peptide substrate as the biorecognition element and the eATRP-based SI-GOP for signal amplification has been described for the signal-on assay of trypsin activity. One key point of the assay is the design of the peptide substrate, which should be carboxyl-group-free and be end-tethered via the N-terminus, such that the tryptic cleavage of peptide substrate can leave the fragment with a free carboxyl terminus on the electrode surface; otherwise, no functional sites are available to conjugate the ATRP initiators via the Zr(IV) linkers. The eATRP-based SI-GOP is easy to operate, highly efficient, tolerant to oxygen, and low-cost as an amplification strategy, through which a large amount of electroactive tags can be introduced within a relatively short grafting time (30 min), allowing the sensitive assay of trypsin activity at a level as low as 0.016 mU mL^{-1} (~2.68 pM or ~0.064 ng mL^{-1}). Such a design that the signal tags are introduced after the substrate cleavage enables the generation of a higher response signal toward a higher level of trypsin activity, leading to a signal-on assay, which is more tolerant to false positives. In addition, this electrochemical trypsin biosensor is highly selective and applicable to inhibitor screening and the assay of trypsin activity in the presence of complex biological matrices, thus showing great promise for diagnostic applications.

Declaration of competing interest

The authors declare that they have no known competing financial interests or personal relationships that could have appeared to influence the work reported in this paper.

CRediT authorship contribution statement

Qiong Hu: Conceptualization, Methodology, Investigation, Writing - original draft, Visualization, Project administration, Funding acquisition. **Yu Bao:** Software, Funding acquisition. **Shiyu Gan:** Data curation, Funding acquisition. **Yuwei Zhang:** Writing - review & editing. **Dongxue Han:** Writing - review & editing. **Li Niu:** Supervision, Funding acquisition.

Acknowledgments

This work was supported by the National Natural Science Foundation of China [21904026], the Project Funded by China Postdoctoral Science Foundation [2018M643040], and the National Natural Science Foundation of China [21974031, 21974032, and 21974033].

Appendix A. Supplementary data

Supplementary data to this article can be found online at https://doi.org/10.1016/j.bios.2020.112358.

References

Aebersold, R., Mann, M., 2003. Nature 422, 198–207.
Adjemian, J., Anne, A., Cauet, G., Demaille, C., 2010. Langmuir 26, 10347–10356.
Anne, A., Chovin, A., Demaille, C., 2012. Langmuir 28, 8804–8813.
Algar, W.R., Malanoski, A.P., Susumu, K., Stewart, M.H., Hildebrandt, N., Medintz, I.L., 2012. Anal. Chem. 84, 10136–10146.
Bi, X., Lai, S.L., Yang, K.L., 2009. Anal. Chem. 81, 5503–5509.
Boyer, C., Corrigan, N.A., Jung, K., Nguyen, D., Nguyen, T.K., Adnan, N.N.M., Oliver, S., Shanmugam, S., Yeow, J., 2016. Chem. Rev. 116, 1803–1949.
Chen, L., Fu, X., Li, J., 2013. Nanoscale 5, 5905–5911.
Cao, Y., Yu, J., Bo, B., Shu, Y., Li, G., 2013. Biosens. Bioelectron. 45, 1–5.
Cheng, M., Zhou, J., Zhou, X., Xing, D., 2018. Sens. Actuators, B 262, 516–521.
Dai, H., Chen, S., Li, Y., Zeng, B., Zhang, S., Hong, Z., Lin, Y., 2017. Biosens. Bioelectron. 92, 687–694.
Elias, E., Wood, T., Redshaw, M., 1977. Lancet 310, 66–68.
Ertürk, G., Hedström, M., Mattiasson, B., 2016. Biosens. Bioelectron. 86, 557–565.
Gu, X., Yang, G., Zhang, G., Zhang, D., Zhu, D., 2011. ACS Appl. Mater. Interfaces 3, 1175–1179.
Goldberg, J.M., Chen, X., Meinhardt, N., Greenbaum, D.C., Petersson, E.J., 2014. J. Am. Chem. Soc. 136, 2086–2093.
González-Fernández, E., Avlonitis, N., Murray, A.F., Mount, A.R., Bradley, M., 2016. Biosens. Bioelectron. 84, 82–88.
He, P., Zheng, W., Tucker, E.Z., Gorman, C.B., He, L., 2008. Anal. Chem. 80, 3633–3639.
Hu, J., Liu, F., Ju, H., 2015. Anal. Chem. 87, 4409–4414.
Hu, Q., Wang, Q., Sun, G., Kong, J., Zhang, X., 2017. Anal. Chem. 89, 9253–9259.
Hu, Q., Wang, Q., Jiang, C., Zhang, J., Kong, J., Zhang, X., 2018. Biosens. Bioelectron. 110, 52–57.
He, M.Q., Chen, S., Yao, K., Meng, J., Wang, K., Yu, Y.L., Wang, J.H., 2019a. Anal. Chem. 92, 1395–1401.
Hu, Q., Kong, J., Han, D., Zhang, Y., Bao, Y., Zhang, X., Niu, L., 2019. Anal. Chem. 91, 1936–1943.
He, P., Lou, X., Woody, S.M., He, L., 2019b. ACS Sens. 4, 992–1000.
Hu, Q., Bao, Y., Gan, S., Zhang, Y., Han, D., Niu, L., 2020a. Anal. Chem. 92, 3470–3476.
Hu, Q., Gan, S., Bao, Y., Zhang, Y., Han, D., Niu, L., 2020b. J. Mater. Chem. B 8, 3327–3340.
Keil, B., 1971. Enzymes 3, 249–275.
Kato, M., Kamigaito, M., Sawamoto, M., Higashimura, T., 1995. Macromolecules 28, 1721–1723.
Kim, S., Sikes, H.D., 2019. ACS Appl. Mater. Interfaces 11, 28469–28477.
Kim, S., Sikes, H.D., 2020. Polym. Chem. 11, 1424–1444.
Long, G.L., Winefordner, J.D., 1983. Anal. Chem. 55, 712A–724A.
Lou, X., Lewis, M.S., Gorman, C.B., He, L., 2005. Anal. Chem. 77, 4698–4705.
Lefkowitz, R.B., Schmid-Schönbein, G.W., Heller, M.J., 2010. Electrophoresis 31, 2442–2451.
Liang, R.P., Tian, X.C., Qiu, P., Qiu, J.D., 2014. Anal. Chem. 86, 9256–9263.
Magenau, A.J., Strandwitz, N.C., Gennaro, A., Matyjaszewski, K., 2011. Science 332, 81–84.
Matyjaszewski, K., Tsarevsky, N.V., 2014. J. Am. Chem. Soc. 136, 6513–6533.
Park, S., Kim, G., Seo, J., Yang, H., 2016. Anal. Chem. 88, 11995–12000.
Raorane, D.A., Lim, M.D., Chen, F.F., Craik, C.S., Majumdar, A., 2008. Nano Lett. 8, 2968–2974.
Sikes, H.D., Hansen, R.R., Johnson, L.M., Jenison, R., Birks, J.W., Rowlen, K.L., Bowman, C.N., 2008. Nat. Mater. 7, 52–56.
Stoytcheva, M., Zlatev, R., Cosnier, S., Arredondo, M., Valdez, B., 2013. Biosens. Bioelectron. 41, 862–866.
Wang, J.S., Matyjaszewski, K., 1995. J. Am. Chem. Soc. 117, 5614–5615.
Wu, Y., Liu, S., He, L., 2009. Anal. Chem. 81, 7015–7021.
Wu, Y., Liu, S., He, L., 2010. Biosens. Bioelectron. 26, 970–975.
Wang, Y., Zhang, Y., Liu, B., 2010. Anal. Chem. 82, 8604–8610.
Wu, Y., Wei, W., Liu, S., 2012. Acc. Chem. Res. 45, 1441–1450.
Wang, C., Ouyang, J., Wang, Y.Y., Ye, D.K., Xia, X.H., 2014. Anal. Chem. 86, 3216–3221.
Wu, P., Zhao, T., Zhang, J., Wu, L., Hou, X., 2014. Anal. Chem. 86, 10078–10083.
Wu, Z., Liu, Y., Liu, Y., Xiao, H., Shen, A., Zhou, X., Hu, J., 2015. Biosens. Bioelectron. 65, 375–381.
Yuan, L., Wei, W., Liu, S., 2012. Biosens. Bioelectron. 38, 79–85.
Zauner, T., Berger-Hoffmann, R., Müller, K., Hoffmann, R., Zuchner, T., 2011. Anal. Chem. 83, 7356–7363.
Zaccheo, B.A., Crooks, R.M., 2011. Anal. Chem. 83, 1185–1188.
Zhang, H., Yu, D., Zhao, Y., Fan, A., 2014. Biosens. Bioelectron. 61, 45–50.
Zeng, T., Zhang, T., Wei, W., Li, Z., Wu, D., Wang, L., Guo, J., He, X., Ma, N., 2015. ACS Appl. Mater. Interfaces 7, 11849–11856.
Zhou, S., Wang, L., Chen, X., Guan, X., 2016. ACS Sens. 1, 607–613.